

# Breakdown of a conservation law in incommensurate systems

L. Consoli, H. J. F. Knops, and A. Fasolino

*Institute for Theoretical Physics, University of Nijmegen, Toernooiveld 1, 6525 ED Nijmegen, The Netherlands*  
(December 2, 2024)

We show that invariance properties of the Lagrangian of an incommensurate system, as described by the Frenkel Kontorova model, imply the existence of a generalized angular momentum which is an integral of motion if the system remains incommensurate. The behavior of this quantity can therefore monitor the character of the system as incommensurate (when it is conserved) or commensurate (when it is not). We find that, during the dynamics, the non-linear couplings of our model cause parametric phonon excitations which lead to the appearance of Umklapp terms and to a sudden deviation of the generalized momentum from a constant value, signalling a dynamical transition from a floating to a pinned state. We point out that this transition is related but does not coincide with the onset of sliding friction which can take place when the system is still incommensurate.

PACS numbers: 05.45.-a, 45.10.-b, 45.05.+x, 81.40.Pq

## I. INTRODUCTION

Measuring friction at an atomic level has recently become experimentally possible [1]. Many studies of the dynamics of appropriate non-linear systems aiming at establishing the mechanisms giving rise to energy dissipation during the sliding of a body onto a crystalline surface have appeared in the literature [2–5]. The Frenkel-Kontorova (FK) model, which describes a harmonic chain interacting with a rigid periodic substrate, is particularly suitable to study the important case of an incommensurate lattice parameter ratio of the contacting surfaces. The ground state properties of this model have been thoroughly studied [6]. At a critical value  $\lambda_c$  of the coupling to the external potential, the ground state of the system displays a structural transition (Aubry transition) from a floating (incommensurate) to a pinned (commensurate) configuration. Below this threshold, the center of mass of the static system can be displaced on the substrate without energy costs. Therefore, one might expect a frictionless regime also in a dynamic situation and a *superlubric* regime, where the chain would slide indefinitely, has been predicted for this case [2]. In a previous paper [5] we have pointed out that the inherent non-linear coupling of the center of mass (CM) motion to the phonons leads instead to an irreversible decay of the CM velocity. The essential mechanism for the transfer of kinetic energy from the center of mass to the internal vibrations is the parametric resonant excitation of phonons mediated by ordinary resonances with phonons related to the modulating potential.

Here we show that this type of mechanism has another important consequence, namely it causes the appearance of Umklapp terms, signalling a dynamical transition in the system from a floating to a pinned state. We have studied this phenomenon by identifying a new quantity, which we call generalized angular momentum (GAM), which is an integral of motion only if the system is incommensurate, reflecting the invariance of the Lagrangian of the model for a phase shift in this state. We show

that this invariance is equivalent to the absence of Umklapp terms. By means of numerical simulations we show that the temporal behavior of the GAM is a powerful probe of the (in)commensurability of the system. Simulations where the incommensurate ground state is given an initial velocity show that the GAM remains conserved up to a well defined time where a sudden jump takes place. We have been able to relate this change of behavior from conserved to non conserved to the appearance of Umklapp terms. An important finding is that this incommensurate-commensurate transition does not coincide with the onset of friction. It was recently suggested by Popov [7] that the appearance of Umklapp terms, i.e. the conservation of quasi-momentum instead of momentum for crystalline systems, is the mechanism via which friction occurs in incommensurate contacts. The present result shows that this is not the only mechanism. By monitoring the incommensurability of the system via the GAM we can show that decay of the CM velocity may occur already in the incommensurate phase. The onset of friction and the appearance of Umklapp terms are both caused by non-linear couplings and resonant phonon excitations in the system but remain two distinct phenomena occurring at different times.

In Sec. II we describe the construction of the GAM by deriving it from the Lagrangian for the system in Fourier space and define conditions under which it is conserved. In Sec. III A we present results of numerical simulations which confirm the validity of our analytical derivation and underline the usefulness of the GAM to discriminate between commensurate and incommensurate systems. Subsequently, we examine in Sec. III B the relationship between commensurability and Umklapp and show the presence of a well-defined transition time. In Sec. IV we present conclusions and perspectives of this work. In the Appendix we provide the reader with an explicit proof that the GAM is an integral of motion in absence of Umklapp.

## II. CONSTRUCTION OF A GENERALIZED ANGULAR MOMENTUM

In this section we will construct a generalized angular momentum for the dynamical FK model, as described in Ref. [5]. We remind the reader that this model represents a chain of  $N$  particles which interact with each other via a first-neighbor harmonic potential and are subjected to an external, spatially periodic, potential of strength  $\lambda$ . The FK Hamiltonian reads:

$$\mathcal{H} = \sum_{n=1}^N \left[ \frac{p_n^2}{2} + \frac{1}{2} (u_{n+1} - u_n - l)^2 + \frac{\lambda}{2\pi} \sin\left(\frac{2\pi u_n}{m}\right) \right] \quad (1)$$

where the  $u_n$  are the particle positions and  $p_n$  their momenta. The ratio between the modulation period of the external potential  $m$  and  $l$  (the equilibrium distance between the atoms of the chain for  $\lambda = 0$ ) is taken to be irrational, i.e. the system is incommensurate. In our calculations we take  $m = 1$  and  $l = \tau = \frac{\sqrt{5}+1}{2}$  (golden mean). In the numerical implementation for a finite system of  $N$  particles we impose periodic boundary conditions

$$u_{N+1} = Nl + u_1 \quad (2)$$

This implies that we have to choose commensurate approximants for the equilibrium distance  $l$ . By expressing  $l$  as ratio of consecutive Fibonacci numbers we obtain approximants which satisfy the condition  $l \times N = M \times 1$  with  $M$  and  $N$  integers. Let us introduce the modulation wavevector  $q = 2\pi l = 2\pi(M/N)$  and the position and momentum of the CM of the chain of atoms:

$$Q = \frac{1}{N} \sum_n u_n, \quad P = \frac{1}{N} \sum_n p_n \quad (3)$$

The equations of motion for the deviations  $x_n = u_n - nl - Q$  from the equilibrium positions in the uncoupled chain are then given by:

$$\ddot{x}_n = x_{n+1} + x_{n-1} - 2x_n + \lambda \cos(qn + 2\pi x_n + 2\pi Q) \quad (4)$$

As noted in Ref. [5], in the weak coupling regime it is useful to move to Fourier coordinates  $x_k = \frac{1}{N} \sum_n e^{-ikn} x_n$  with  $k = 2\pi K/N$ . The phonon dispersion of the chain for  $\lambda = 0$  is denoted by  $\omega_k \equiv \omega(k) = 2|\sin(k/2)|$ . The Lagrangian associated with Eq. (1) in transformed space becomes:

$$\mathcal{L} = N \left( \sum_k \left( \frac{1}{2} \dot{x}_k \dot{x}_{-k} - \frac{1}{2} \omega_k^2 x_k x_{-k} \right) + \frac{\lambda}{2\pi} \frac{1}{2i} \sum_{m=1}^{\infty} \frac{(i2\pi)^m}{(m!)} \times \sum_{k_1 \dots k_m} (e^{i2\pi Q} x_{k_1} \dots x_{k_m} \delta_{k_1 + \dots + k_m, -q} - \right.$$

$$\left. - (-1)^m e^{-i2\pi Q} x_{k_1} \dots x_{k_m} \delta_{k_1 + \dots + k_m, q} \right) + \frac{1}{2} (\dot{Q})^2 \quad (5)$$

It is important to notice that since wave vectors are defined modulo  $2\pi$ , the Kronecker deltas in Eq. (5) should be read as:

$$k_1 + k_2 + \dots + k_m = q + s \times 2\pi \quad (6)$$

Umklapp is present whenever this relation is satisfied with  $s \neq 0$ . It is clear that the occurrence of Umklapp depends on the modes  $x_k$  which are not negligible, and on the choice of the (extended or reduced) Brillouin zone in which  $k$  is represented. It is known that in the groundstate, for a coupling  $\lambda$  well below the critical value  $\lambda_c$ , which for this model assumes the value  $\lambda_c = 0.154\dots$ , the modes with wavevector  $nq$  have an amplitude which scales as  $\lambda^{|n|}$ . This number  $|n|$  is therefore a natural label to represent the modes; we define  $n(k, q)$  as the smallest (in absolute value) number which satisfies:

$$k = n(k, q)q \bmod(2\pi) \quad (7)$$

For a finite system with  $N$  particles, where  $k$  can be represented in the reduced Brillouin zone as  $k = K(2\pi/N)$ ,  $K \in (-1/2N, 1/2N]$ , this can be rewritten as:

$$K = nM \bmod(N), \quad n \in (-1/2N, 1/2N] \quad (8)$$

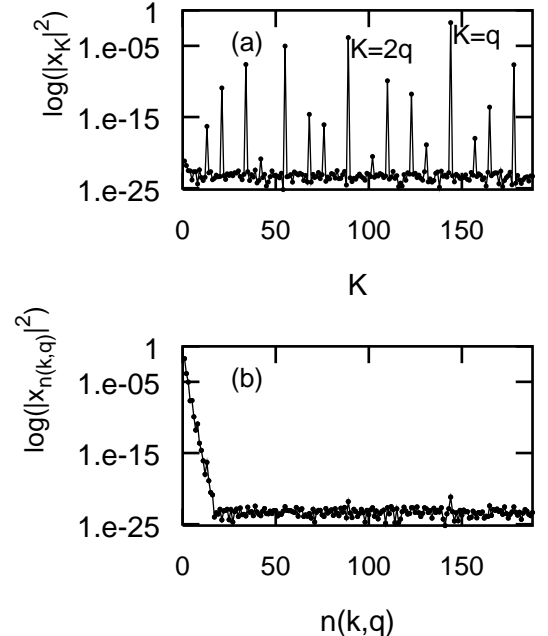


FIG. 1. FK model for  $N = 377$ ,  $\lambda = 0.05$ . (a) Phonon amplitudes squared plotted as a function of the wavevector  $K$ , as in Eq. (8). The first two  $nq$  modes are explicitly indicated. (b) Same as in panel (a), relabeled according to Eq. (7). Due to finite numerical precision, the exponential decay with  $\lambda^{|n|}$  is apparent only for the first fifteen modes.

In Fig. 1 we compare the phonon amplitudes for the ground state of the FK model for  $N = 377$ ,  $\lambda = 0.05$ , plotted as a function of the usual wavevector label  $K$  (panel (a)), as well as reordered according to the label  $n$  (panel (b)). Note that, due to finite numerical precision, the scaling behavior is hidden in numerical noise after the first fifteen modes.

The use of  $n$  as a mode label makes apparent the fact that there is no Umklapp in the ground state of the FK model in the modulated (or incommensurate) phase for  $\lambda < \lambda_c$ . In fact Umklapp would imply the presence of a non vanishing term:

$$x_{n_1 q} x_{n_2 q} \cdots x_{n_m q}; \quad n_1 + n_2 + \cdots n_m = sN \quad \text{with } s \neq 0 \quad (9)$$

The joint amplitude of this term would be:

$$\lambda^{|n_1| + \cdots |n_m|} \leq \lambda^{|s|N} \quad (10)$$

which vanishes for  $N \rightarrow \infty$ .

The absence of Umklapp terms is directly related to the existence of a free floating phase, which is a well known invariance property of the FK model. In the present notation it amounts to the invariance of the Lagrangian for the transformation:

$$Q \rightarrow Q + q\phi/2\pi \quad (11)$$

$$x_k \rightarrow x_k e^{ik\phi} \quad (12)$$

Having found an invariance for the Lagrangian, we can look for the conjugate conserved momentum. We get:

$$p_\phi = \frac{\partial \mathcal{L}}{\partial \dot{\phi}} = -i \sum_n n q x_{-nq} \dot{x}_{nq} + \frac{q}{2\pi} \dot{Q} \equiv L + \frac{q}{2\pi} \dot{Q} \quad (13)$$

The quantity  $p_\phi$  represents a generalized angular momentum (GAM). It is important to realize that the invariance of the Lagrangian only holds in a subspace of the full phase space where Umklapp terms can be neglected as it is the case for the floating (incommensurate) ground state. In order to stress this point, a direct calculation of  $\dot{p}_\phi$  is given in the Appendix, showing that the GAM  $p_\phi$  is an integral of motion only if Umklapp is not present.

This quantity is therefore an useful tool to discriminate between commensurate and incommensurate structures. In the next section we present numerical simulations that we carried out for various values of the parameters of the model, showing how  $p_\phi$  is a good indicator of the (in)commensurate character of the system under examination.

### III. NUMERICAL RESULTS

#### A. Commensurate vs. incommensurate

We have performed numerical simulation in order to study the behavior of the GAM, as defined by Eq. (13),

integrating by a Runge-Kutta algorithm the  $N$  Eqs. (4). We assign to the particles of the chain as initial conditions momenta  $p_n = P_0$  and positions  $x_n(t=0)$  corresponding to the ground state.

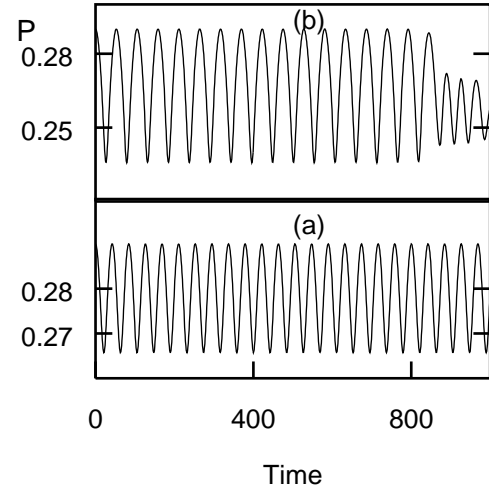


FIG. 2. Behavior of the CM momentum  $P$  for: (a) an incommensurate configuration with  $N = 144$ ,  $\tau = 233/144$ ,  $\lambda = 0.015$ ,  $P_0 = 0.29$ ; (b) a commensurate case with  $N = 144$ ,  $\tau = 5/3$ ,  $\lambda = 0.015$ ,  $P_0 = 0.29$ . Note the qualitative similarity in the behavior of  $P$ .

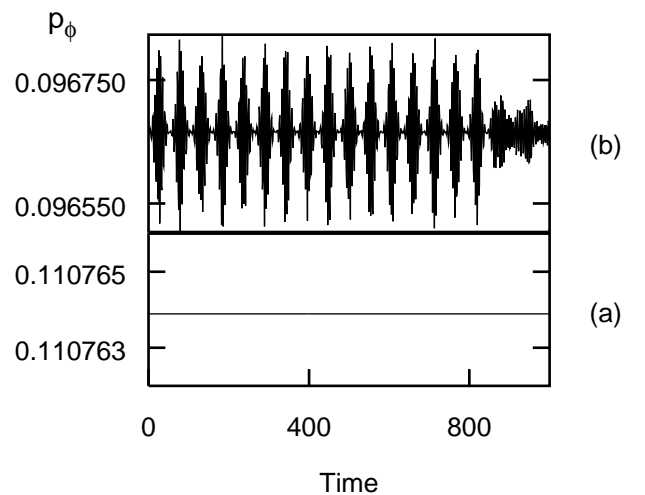


FIG. 3. Behavior of  $p_\phi$  for the parameters of the model as described in Fig. 2. (a) Incommensurate case: the GAM is constant within numerical precision. (b) Commensurate case: the GAM is not conserved. Note the change of scale going from panel (a) to panel (b).

Fig. 2 shows simulation results for the same number of particles  $N$  and potential strength  $\lambda$ , but for a low ( $\tau = 5/3$ ) and a high ( $\tau = 233/144$ ) approximant to the golden mean  $\tau$ , producing an approximate incommensurate structure and a commensurate one. The qualitative behavior of the momentum of the center of mass  $P$  is similar, whereas the behavior of  $p_\phi$  in Fig. 3 is remarkably different being conserved only for the case which approximates an incommensurate system. This confirms that  $p_\phi$  can be used as a tool to discriminate unambiguously between commensurate and incommensurate structures.

Furthermore, our numerical simulations show a remarkable fact. If we start the simulation with an incommensurate initial condition,  $p_\phi$  is indeed conserved, but only up to a critical time  $t_c$ , after which it rapidly deviates from its initial conserved value. This is shown in Fig. 4, where we can examine the behavior of  $p_\phi$  and  $P$  in a weak coupling, highly incommensurate ( $\tau = 610/377$ ,  $\lambda = 0.015$ ) case. In order to check that the observed variation of  $p_\phi$  only sets in after a critical time  $t_c$ , we have analyzed the behavior of the quantity  $\log(p_\phi - C_0)$ ,  $C_0$  being the value of  $p_\phi$  at  $t = 0$ . It is evident from panel (c) of Fig. 4 that we can identify such a critical time  $t_c$  where the GAM has a jump in value of various order of magnitude. Besides, this figure shows that, for  $t < t_c$ ,  $p_\phi$  is conserved within our numerical accuracy, never exceeding variation larger than  $10^{-20}$ . A new question arises, namely: how can we explain the time variation of  $p_\phi$ , considering the fact that we started from an incommensurate configuration? We show in the next section that the answer lies in the appearance of Umklapp terms, which render the system commensurate, thus leading to a non conservation of  $p_\phi$ .

## B. The role of Umklapp processes

As we have pointed out in Sec. II,  $p_\phi$  is conserved only in the absence of Umklapp, that is to say when terms of the form given in Eq. (9) have a vanishing amplitude for  $N \rightarrow \infty$ . As we have seen, this is the case for the groundstate of the incommensurate system. However, starting from the ground state, this may change during the dynamics due to parametric resonances. The movement of the CM with velocity  $P$  induces a modulation with frequency  $\Omega = 2\pi P$  in the equations of motion of the system. Linear stability analysis [4,5] shows that a mode  $k$  grows exponentially (with rise time  $\tau$ ) whenever its frequency satisfies:

$$\Omega \simeq \frac{\omega(k) + \omega(mq - k)}{m} \quad (14)$$

for some  $m$ . The  $\simeq$  symbol indicates an instability window of relative width  $w_m$  that scales with  $\lambda^{|m|}$ .

Suppose now that a mode  $x_k$  is unstable. Let  $n(k, q)$  be its label according to Eq. (7). When  $n(k, q) = \mathcal{O}(N)$ , this mode could lead to Umklapp as soon as its amplitude becomes finite. However, since its initial value is

of order  $\lambda^{|n|}$ , it requires an infinite amount of time (as  $N \rightarrow \infty$ ) to render  $\lambda^{|n|}e^{t/\tau}$  finite. So we have to look for modes  $k$  in the instability windows with  $n(k, q)$  finite. Since the mapping  $n(k, q) \rightarrow k$  leads to a uniform distribution, one indeed expects to find such a  $k$  with  $|n(k, q)| < 1/w$ , where  $w = \sum_m w_m$  is the relative width of the joint instabilities windows. Once the amplitude of the mode  $k$  starts growing (with a behavior given by an exponential law of the form:  $Ae^{t/\tau}$ , with  $A$  bounded from below via the upper bound on  $n$ ), also modes  $k'$  with  $n'(k', q) = pn(k, q) \pm 1, p = 2, 3, \dots$  start to develop via non linear terms in the equations of motion (see Ref. [5] for details), with the form:

$$x'_k \simeq \lambda(Ae^{t/\tau})^p \quad (15)$$

Umklapp can result when repeating this process  $\mathcal{O}(N)$  times (i.e., when  $pn \sim N$ ) still gives a finite result. From Eq. (15) it is clear that this will happen when  $x_k(t)$  exceeds some threshold value, which is the case for  $t$  larger than the critical time  $t_c$  introduced in Sec. III A.

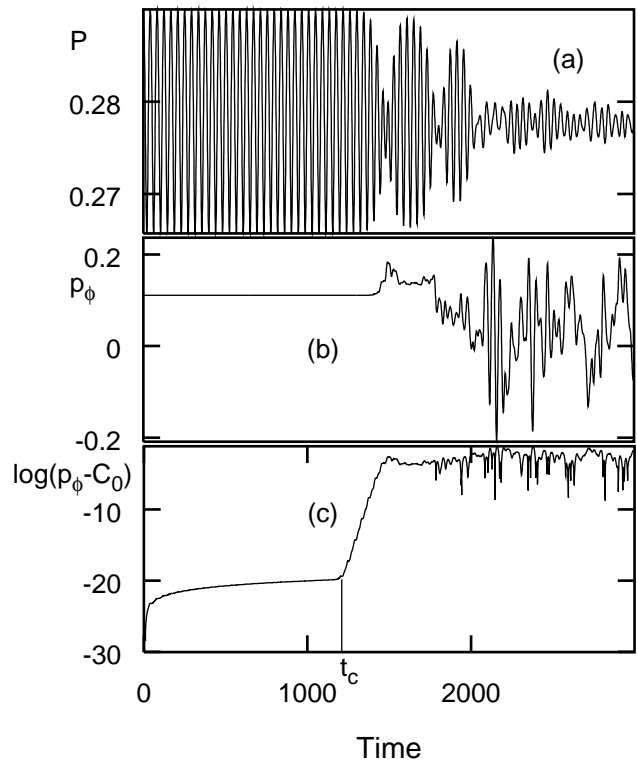


FIG. 4.  $N = 377$ ,  $\tau = 610/377$ ,  $\lambda = 0.015$ ,  $P_0 = 0.29$ . (a) Behavior of the CM momentum  $P$ . (b) Behavior of  $p_\phi$ . It is possible to see how the GAM stops being conserved. (c) In order to check if there is a critical time  $t_c$ , we plot the quantity  $\log(p_\phi - C_0)$ , where  $C_0 = p_\phi(t = 0)$ . We show that  $t_c$  can be unambiguously identified. Note that, even if, in this weak coupling case, the decay of the CM coincides with the breakdown of conservation of  $p_\phi$ , this is not always the case. See also text and Fig. 6.

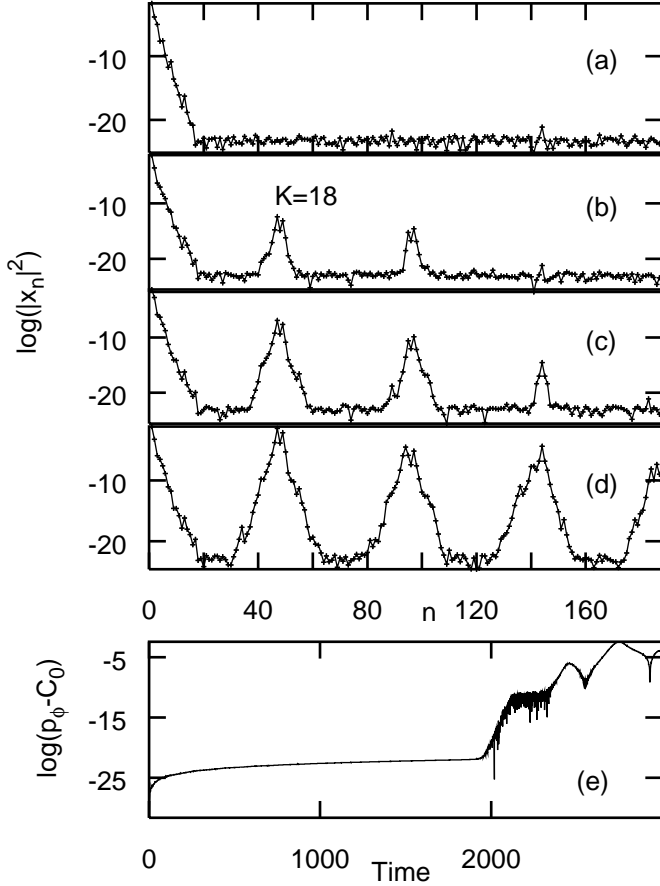


FIG. 5.  $N = 377$ ,  $\tau = 610/377$ ,  $\lambda = 0.05$ ,  $P_0 = 0.15$ . The appearance of Umklapp terms is shown. (a) Phonon amplitudes squared at  $t = 0$ . (b) Same at  $t = 1000$ . The mode  $K = 18$  ( $n = 47$ ) is starting to grow; (c) Same at  $t = 1500$ . The modes with  $n \times 47$ , with  $n = 1, 2, 3$  are all present, but there is still no Umklapp. (d) The mode with  $K = 18$  has become order unity and Umklapp appears, signalled by the excited modes at the zone boundary. (e) Time evolution of  $\log(p_\phi - C_0)$ . The appearance of Umklapp in panel (e) corresponds to the breakdown of the conservation of the GAM. See also text for a detailed explanation of the Umklapp mechanism.

Fig. 5 shows this mechanism at work: here we have taken  $P_0 = 0.15$ , so that  $\Omega = 2\pi P = \omega_q/2$ , and  $N = 377$  ( $\tau = 610/377$ ). For this value of  $\Omega$  Eq. (14) has approximate solutions for  $n = 2$  for  $k = K(2\pi/N)$ , with  $K = 18, 19$ . The corresponding values for  $n(k, q)$  are in the case  $n(18, q) = 47$  and  $n(19, q) = 97$ . Panel (a) shows that the phonon amplitudes at  $t = 0$  decay indeed exponentially with  $n$ . Panel (b) shows that the unstable mode  $K = 18$  with the lowest value of  $n$  starts to grow at  $t = 1000$ . Modes at  $n = 2 \times 47$  are also present, due to non linear terms, but quadratically smaller, as explained above. At  $t = 1500$  modes at  $n = 3 \times 47$  become visible, as shown in panel (c). There is still no Umklapp, as can

be seen from the absence of an amplitude at the zone boundary. Such a term, corresponding to  $n = 4 \times 47$ , finally appears in panel (d), at  $t = 2000$ . Indeed, this is also precisely the time at which  $|x_{18}|^2$  becomes order unity and  $p_\phi$  stops being conserved (see panel (e)).

The mechanism described above shows that the appearance of Umklapp terms causes a sudden transition from an incommensurate to a commensurate structure. In this respect, this transition represents a dynamical analogue of the transition from a floating to a pinned state taking place in the static model at  $\lambda_c$ . The important difference is that, for the dynamical case, this transition occurs as a function of time at all values  $\lambda < \lambda_c$ .

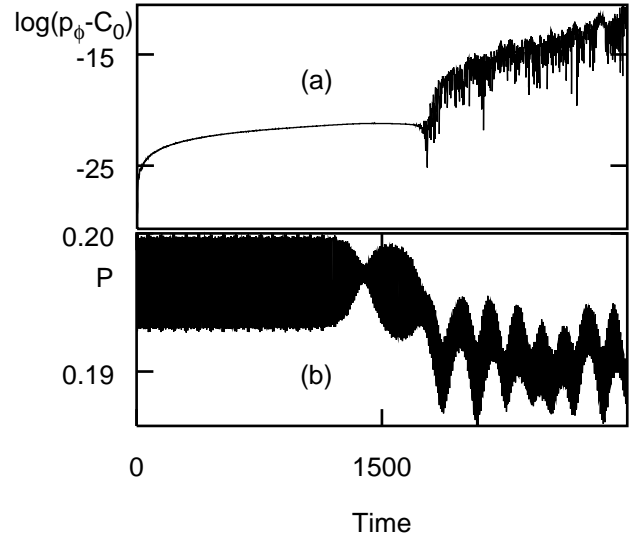


FIG. 6.  $N = 144$ ,  $\tau = 233/144$ ,  $\lambda = 0.05$ ,  $P_0 = 0.20$ . (a) Time evolution of  $\log(p_\phi - C_0)$ . (b) CM momentum  $P$ . Note that the CM momentum has begun its decay before the deviation of  $p_\phi$  from its constant value occurs.

Before concluding this section it is important to discuss the relation between the dynamical incommensurate-commensurate transition described above and the onset of friction. The onset of friction is driven by the coupling of the CM to the mode with the modulation wavevector  $q$  or its harmonics and consists in a special kind of parametric resonances involving more than one phonon and where the time dependent driving terms are themselves in resonance [5]. The appearance of Umklapp requires instead a phonon with finite amplitude and very special (zone boundary) wavevector. We could say that the last process is more difficult to achieve. In Fig. 6, it can be seen that the GAM stays conserved, even after the CM momentum has begun its decay. This means that there is an interval of time in which the first mechanism is active whereas the second has not yet taken place. We can identify two times: one which characterizes the onset of friction and one which describes the commensuration of the system. In this respect the dynamical model is much

richer than the static one. At the Aubry transition, the appearance of a static friction occurs at the same value of  $\lambda$  at which the system gets pinned.

#### IV. CONCLUSIONS

We have shown, in the framework of the undamped 1D dynamical FK model, that it is possible to obtain analytical results concerning the existence of a new integral of motion which represents a generalized angular momentum related to a phase invariance in incommensurate systems, and we have confirmed this finding by means of numerical simulations. We have also shown that, during the dynamics, a breakdown of the conservation of the GAM occurs at a well-defined time, signalling an incommensurate-commensurate dynamical transition. We have been able to prove that this transition is related to the appearance of Umklapp processes, caused by non linear couplings of the system. We are currently trying to further characterize the nature (order) of the transition of the dynamical model. We have furthermore shown that the onset of friction and the commensuration of the system are related but distinct phenomena occurring in general at different times, which we have been able to identify.

#### ACKNOWLEDGEMENTS

We would like to thank Ted Janssen for interesting discussions and suggestions.

#### APPENDIX:

We are going to provide in this appendix an explicit derivation that  $\dot{p}_\phi = 0$ . Let us consider the first term on the right hand side of Eq. (13):

$$L = -i \sum_n nq x_{-nq} \dot{x}_{nq} \quad (\text{A1})$$

In order to simplify the notation, we will adopt from now on the following convention:  $nq \equiv \kappa$ . Take the derivative of Eq. (A1):

$$\dot{L} = -i \sum_{\kappa} \kappa x_{-\kappa} \ddot{x}_{\kappa} - i \sum_{\kappa} \kappa \dot{x}_{-\kappa} \dot{x}_{\kappa} \quad (\text{A2})$$

We can immediately see that for symmetry reasons the second term cancels. Let us now take the equation for  $\ddot{x}_\kappa$  as follows from the Euler-Lagrange equations:

$$\ddot{x}_\kappa = -\omega_\kappa^2 x_\kappa + \frac{\lambda}{2} \sum_{m=0}^{\infty} \frac{(i2\pi)^m}{m!} \sum_{\kappa_1 \dots \kappa_m} [e^{i2\pi Q} x_{\kappa_1} \dots x_{\kappa_m} \delta_{\kappa_1 + \dots + \kappa_m, -q + \kappa} + (-1)^m e^{-i2\pi Q} x_{\kappa_1} \dots x_{\kappa_m} \delta_{\kappa_1 + \dots + \kappa_m, q + \kappa}] \quad (\text{A3})$$

and the equation for the CM motion:

$$\ddot{Q} = \frac{\lambda}{2} \sum_{m=1}^{\infty} \frac{(i2\pi)^m}{m!} \sum_{\kappa_1 \dots \kappa_m} [e^{i2\pi Q} x_{\kappa_1} \dots x_{\kappa_m} \delta_{\kappa_1 + \dots + \kappa_m, -q} + (-1)^m e^{-i2\pi Q} x_{\kappa_1} \dots x_{\kappa_m} \delta_{\kappa_1 + \dots + \kappa_m, q}] \quad (\text{A4})$$

Let us insert Eq. (A3) in Eq. (A2). We get:

$$\dot{L} = -i \left\{ \frac{\lambda}{2} \sum_{m=0}^{\infty} \frac{(i2\pi)^m}{m!} \times \sum_{\kappa, \kappa_1, \dots, \kappa_m} [e^{i2\pi Q} \kappa x_{-\kappa} x_{\kappa_1} \dots x_{\kappa_m} \delta_{\kappa_1 + \dots + \kappa_m, -q + \kappa} + \dots] \right\} \quad (\text{A5})$$

(Note that the first term in Eq. (A3) cancels for the same symmetry reasons given above). We have for simplicity explicitly written down only the first part of the expression in square brackets, since we treat the second part exactly in the same way. Rearranging the delta function and applying the following symmetry transformation:

$$\kappa x_{-\kappa} \delta_{-\kappa} \rightarrow -\kappa x_{\kappa} \delta_{\kappa} \quad (\text{A6})$$

Eq. (A5) becomes:

$$\dot{L} = -i \left\{ \frac{\lambda}{2} \sum_{m=0}^{\infty} \frac{(i2\pi)^m}{m!} \times \sum_{\kappa, \kappa_1, \dots, \kappa_m} [e^{i2\pi Q} (-\kappa) x_{\kappa} x_{\kappa_1} \dots x_{\kappa_m} \delta_{\kappa + \kappa_1 + \dots + \kappa_m, -q} + \dots] \right\} \quad (\text{A7})$$

Because there is no preferential order in the  $\kappa$ -summation, the following equality holds:

$$(-\kappa) x_{\kappa} x_{\kappa_1} \dots x_{\kappa_m} = (-\kappa_1) x_{\kappa_1} x_{\kappa} \dots x_{\kappa_m} = \dots = (-\kappa_m) x_{\kappa_m} x_{\kappa} \dots x_{\kappa_{m-1}} \quad (\text{A8})$$

There are  $(m+1)$  possibilities, thus we can make the substitution:

$$\kappa = \frac{\kappa + \kappa_1 + \dots + \kappa_m}{m+1} \quad (\text{A9})$$

Therefore, Eq. (A5) becomes:

$$\dot{L} = -i \left\{ \frac{\lambda}{2} \sum_{m=0}^{\infty} \frac{(i2\pi)^m}{m!} \sum_{\kappa, \kappa_1, \dots, \kappa_m} \left[ \left( -\frac{\kappa + \kappa_1 + \dots + \kappa_m}{m+1} \right) e^{i2\pi Q} x_{\kappa} x_{\kappa_1} \dots x_{\kappa_m} \delta_{\kappa + \kappa_1 + \dots + \kappa_m, -q} + \dots \right] \right\} \quad (10)$$

Now, under the assumption that there is no Umklapp  $\kappa_1 + \dots + \kappa_m = q$  and can be taken outside the summation. Hence, we get:

$$\dot{L} = -\frac{q}{2\pi} \left\{ \frac{\lambda}{2} \sum_{m=0}^{\infty} \frac{(i2\pi)^{m+1}}{(m+1)!} \sum_{\kappa, \kappa_1, \dots, \kappa_m} e^{i2\pi Q} x_{\kappa_1} \dots x_{\kappa_m} \delta_{\kappa + \kappa_1 + \dots + \kappa_m, -q} + \dots \right\} \quad (11)$$

The expression in parenthesis is precisely Eq. (A4) for  $\ddot{Q}$  multiplied by  $q/2\pi$ . Hence, we find:

$$\dot{p}_{\phi} = \dot{L} + \frac{q}{2\pi} \ddot{Q} = 0 \quad (12)$$

- [1] C. M. Mate, G. M. McClelland, R. Erlandsson, and S. Chiang, Phys. Rev. Lett. **59**, 1942 (1987); J. Krim, D. H. Solina, and R. Chiarello, Phys. Rev. Lett. **66**, 181 (1991); J. B. Sokoloff, J. Krim, and A. Widom, Phys. Rev. B **48**, 9134 (1993).
- [2] K. Shinjo and M. Hirano, Surf. Sci. **283**, 473 (1993).
- [3] *Physics of Sliding Friction*, edited by B. N. J. Persson and E. Tosatti (Kluwer, Dordrecht, 1996).
- [4] T. Strunz and F.-J. Elmer, Phys. Rev. E **58**, 1601 (1998); **58**, 1612 (1998).
- [5] L. Consoli, H. J. F. Knops, and A. Fasolino, Phys. Rev. Lett. **85**, 302 (2000).
- [6] M. Peyrard and S. Aubry, J. Phys. C **16**, 1953 (1983), and references therein; S. Aubry and L. de Seze, Festkörperprobleme **XXV**, 59 (1985).
- [7] V. L. Popov, Phys. Rev. Lett. **83**, 1632 (1999).